Engineering Structures 111 (2016) 233–245

Contents lists available at ScienceDirect

Engineering Structures

journal homepage: www.elsevier.com/locate/engstruct

Behavior and failure mechanisms of masonry-infilled RC frames (in low-rise buildings) subject to lateral loading

Syed Humayun Basha, Hemant B. Kaushik *

Dept. of Civil Engineering, Indian Institute of Technology Guwahati, Guwahati 781039, India

ARTICLE INFO

Article history:
Received 7 February 2015
Revised 18 December 2015
Accepted 22 December 2015
Available online 6 January 2016

Keywords:
Ductile and non-ductile RC frame
Shear failure
Masonry infill
Fly ash bricks
Seismic design
Strong frame-weak infill

ABSTRACT

The behavior of eleven half-scale, single-story masonry infilled reinforced concrete (RC) frames under slow cyclic in-plane lateral loading was experimentally studied in two stages. Results obtained in the first stage (eight frames) showed that the frames infilled with full-scale and half-scale bricks exhibited higher strength, stiffness, and energy dissipation than their bare frame counterparts. In most cases, columns failed in shear even though the masonry used was quite weak. In order to delay the shear failure in columns, shear design of columns was enhanced as per the existing earthquake standards, and tests were repeated on three improved frames in the second stage. Though shear failure in columns of the improved frames occurred at higher drift level, the shear failure in columns could not be prevented showing the inadequacy of current design codes. Based on the experimental results, an idealized load–displacement relationship for masonry infilled RC frames was developed for different performance levels.

1. Introduction

Masonry walls are generally used as infills in reinforced concrete (RC) frames without accounting for their resistance to lateral loads under strong ground motions. RC frames are designed to exhibit flexural behavior under seismic actions, and when infills are introduced, though the lateral strength, stiffness and energy dissipation capacity of the frames are improved, the lateral load resistance is mostly dominated by shear behavior of columns. A comprehensive review [1–5] of past research on evaluation of lateral load behavior of masonry infilled frames showed that when the strength and stiffness of infill is sufficiently large, local detrimental effect of infill may cause shear failure of columns. Most of the past experimental studies [6–9] reported shear failure of columns in frames not designed as per the recommendations of prevalent seismic standards. From the past studies [9–13], it was observed that there are several factors that had significant influence on failure mechanism of masonry infilled RC frames, which include aspect ratio, openings in the infill panels, column to beam stiffness ratio, axial load ratio on columns, type of infill and the construction methodology, number of stories and bays, etc. Asteris et al. [10] classified failure of infilled frames into five distinct modes (corner crushing, diagonal compression, sliding shear, diagonal cracking, and frame failure) based on the past experimental and analytical studies [14,15], and it was reported that the frame failure mode, associated with weak frame-strong infill configuration, was particularly important. To address this problem, Eurocode 8 [16], ASCE 41 [17], MSJC [18], and Moretti et al. [19] recommended methods to evaluate the shear demand on columns taking into account the effect of infill. A few analytical studies [20,21] were also carried out to predict the shear failure of columns in infilled frames, but such prediction methods may not provide realistic results due to modeling complexities. From the recommendations of the past studies, it is understood that infilled frames need to be designed to resist the excessive shear force from infill.

In order to evaluate the effectiveness of these recommendations, and to understand the failure mechanisms of such frames, an experimental study was undertaken in which half-scale RC frames designed using the current seismic standards were tested. It was also observed that most past studies [19–25] used solid clay or fly ash bricks, hollow blocks or concrete bricks/blocks as infills. In the current study, frames were infilled with fly ash bricks, which were found to be significantly softer and weaker in comparison to the RC frame [22]. This article mainly focuses on evaluating the lateral load behavior of infilled frames of strong frame-weak infill configuration. Effectiveness of design provisions in earthquake standards in improving the shear behavior of RC columns in such frames was also evaluated. Further, effect of T-beam action provided by RC slab on behavior of RC beams was assessed, as most

* Corresponding author. Tel.: +91 361 2582427.
E-mail addresses: s.basha@iitg.ac.in (S.H. Basha), hemantbk@iitg.ac.in (H.B. Kaushik).

http://dx.doi.org/10.1016/j.engstruct.2015.12.034
0141-0296/

of the past studies did not consider stiffening effect of slab and reported failure of beams and beam–column joints.

2. Description of RC frames studied

Half-scale models of an exterior ground-story frame of a two-story office building in Assam, which is one of the most seismic-prone regions in India, have been studied. The effect of RC slab on behavior of the specimens was observed by providing slab over the beam and extending it over a width of 400 mm on both sides of the frame (Fig. 1). Columns of the specimens were constructed on a RC beam of size 400 × 350 mm to provide fixity at the base. Columns were supported laterally using roller bearing steel frames on either side to prevent out-of-plane response of the specimens during in-plane loading. Vertical load applied to the specimens was calculated based on the tributary area above the frame in the storey above it. The total vertical load was applied by placing RC plates on the RC slab, corresponding to an axial load ratio ($P/f_{ck}A_g$) of about 1% on each column of the frame, where P, f_{ck} and A_g represent the axial load, compressive strength of concrete cubes at 28 days, and gross area of column section, respectively. Due to laboratory constraints, no vertical load was applied on the columns and it is not a major deviation from the prototype loading distribution as the vertical load acting on the columns due to upper story was quite low. The stiffening action provided by the RC beam-slab was quite high, and moreover, infill wall was constructed after the casting of the frame. This type of construction practice apparently leaves a gap between the soffit of the beam and the infill wall. Therefore, it was unlikely that the vertical loads applied over the slab were transferred to the infill wall below.

It has been observed in past studies [6–9] that shear demand on RC columns of masonry infilled RC frames is very high, due to the interaction between frame and infill, for which the columns are generally not designed. It was observed that the shear failure of columns may be either due to interaction of columns with strong and stiff infills which may shear-off weak columns in ground storey where contact is only on one-side, or may be due to the column is intact with infill over a partial height creating captive column effect by decreasing the effective length of the column to resist the entire inter-storey drift.

Currently, three Indian standards deal with the design [26,27] and detailing [28] of reinforced concrete members of which IS 456 [26] deals with the general design considerations of reinforced concrete members, IS 1893 [27] with the calculation of earthquake forces and IS 13920 [28] with the ductile detailing of RC structures subjected to seismic forces. The prototype structure considered in the study was designed for the lateral forces corresponding to the highest seismic zone in India but not detailed as per the ductile detailing guidelines [28] (design lateral shear was about 15% of the seismic weight). In order to evaluate the effectiveness of ductile detailing, two types of frames (ductile and non-ductile) were designed in the current study. Reinforcement in RC beam and columns of the non-ductile bare frame specimen was not detailed to exhibit ductility. The design of non-ductile bare frame was similar to that of the ordinary moment frames designed in accordance with ACI 318 [29] and also to the frame designed according to Eurocode 8 [16] without following the detailing requirements for local ductility. The ductile detailing code of India (IS 13920) requires providing special confining reinforcement in the expected plastic hinge locations in beams and columns. However, in ductile bare frame the reinforcement was detailed in accordance with IS 13920 but without provision of special confining reinforcement. Design of ductile bare frame corresponds to special moment resisting frame as per ACI 318 [29] without considering the effect of discontinued stiff members, and it also corresponds to the frame designed for high ductility class in accordance with Eurocode 8 [16], without considering the local effects due to masonry infill.

Table 1 gives the details of the test specimens and reinforcement detailing of ductile and non-ductile frame is shown in Fig. 2. Major distinctions between ductile and non-ductile frames were: spacing of shear reinforcement, bending of hooks, and embedment of ends of shear reinforcement bars into the core concrete. The longitudinal reinforcement remained same in both ductile and non-ductile frames and the members framing into joints were detailed as continuous members. In case of non-ductile frames, shear reinforcement in columns at critical locations (up to 500 mm from the face of top and bottom beams) consisted of 3-legged, 6 mm diameter bars with 90° hooks at 110 mm spacing (Fig. 2(b)). Whereas, in case of ductile frames, similar shear reinforcement in columns was placed with 135° hooks at 90 mm spacing, and embedment length of 10 times bar diameter (Fig. 2(a)).

The experimental study was carried out in two stages: eight specimens were tested in the first stage considering different reinforcement detailing in RC members and using different size bricks for masonry. Three specimens were tested in the second stage to study the influence of providing special confining reinforcement required as per IS 13920 [28]. Two different size of fly ash bricks: full-scale

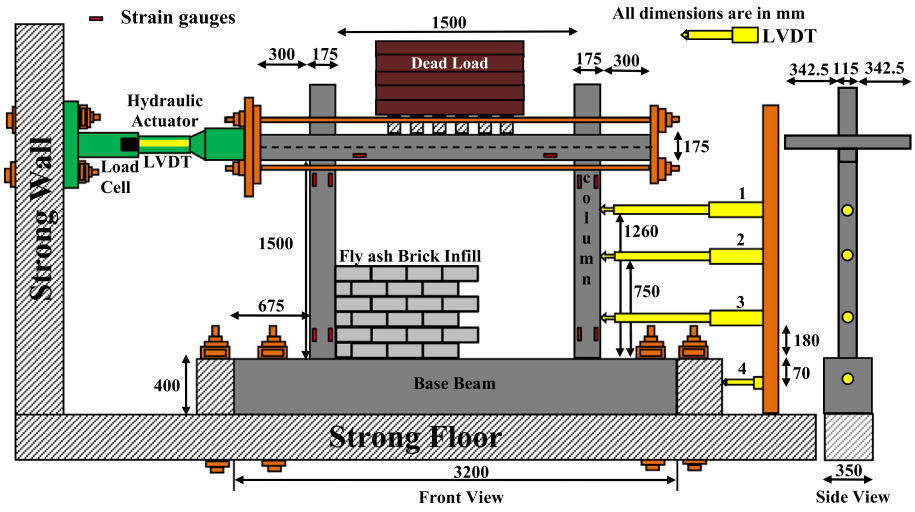

Fig. 1. Details of experimental set up and instrumentation.

Table 1
Details of test specimens.

Specimen no.	Type of frame	Notations	Ductile detailing	Type of masonry
Stage I				
1	Ductile bare frame	DB	Yes	No infill
2	Non-ductile bare frame	NDB	No	No infill
3	Ductile frame infilled with full-scale bricks	DFS	Yes	Full-scale bricks
4	Non-ductile frame infilled with full-scale bricks	NDFS	No	Full-scale bricks
5	Ductile retrofitted frame infilled with full-scale bricks	DRFS	Yes	Full-scale bricks
6	Non-ductile retrofitted frame infilled with full-scale bricks	NDRFS	No	Full-scale bricks
7	Ductile frame infilled with half-scale bricks	DHS	Yes	Half-scale bricks
8	Non-ductile frame infilled with half-scale bricks	NDHS	No	Half-scale bricks
Stage II: Ductile infilled frame				
9	Improved detailing along full column length	DISTL	Yes	Full-scale bricks
10	Improved detailing in critical regions	DISC	Yes	Full-scale bricks
11	Improved detailing in critical regions using high strength bars	DISCSB	Yes	Full-scale bricks

Key: D – Ductile; ND – Non-ductile; B – Bare; FS – Full-scale bricks; HS – Half-scale bricks; R – Retrofitted; I – Improved; S – Shear capacity; TL – Throughout Length; C – Critical regions; SB – High strength bars.

($230 \times 110 \times 75$ mm) and half-scale ($115 \times 55 \times 38$ mm) were used as infill constructed using 1:4 (cement:sand) mix mortar with a water cement ratio of 0.6. Infill wall was constructed by laying bricks in two different patterns: Stretcher bond (running bond) in case of full-scale bricks and English bond in case of half-scale bricks in order to maintain similar thickness of infill in both full-scale and half-scale brick specimens. An aspect ratio (h/l) of 1.0 was considered keeping in view the general room sizes in apartment-type buildings (3 m × 3 m with 3 m high floors). Further, in order to study effectiveness of a commonly adopted retrofitting method, damaged ductile and non-ductile infilled frames (Specimens 3 and 4) were retrofitted by replacing the damaged concrete after welding additional reinforcement in the region where bars had yielded (Specimens 5 and 6). A comparative performance assessment of all the specimens is carried out in the following sections.

3. Material properties

Material properties were evaluated using relevant standards by conducting tests on masonry and its constituents, concrete, and reinforcing bars (Table 2). The average compressive cube strength of concrete (f_{ck}) was 22.4 MPa with modulus of elasticity E_c of about 23700 MPa. Average compressive strength of fly ash brick units (f_b) and mortar cubes (f_j) was about 5.7 MPa and 17.3 MPa, respectively, with modulus of elasticity as 3900 MPa (E_b) and 7400 MPa (E_j), respectively. The compressive masonry prism strength (f'_m) was about 3.9 MPa with modulus of elasticity E_m as 2700 MPa. The average shear strength of masonry wallettes (f'_v) was found to be 0.14 MPa with shear modulus G_m as 730 MPa. Failure of both fly ash brick masonry prisms and fly ash brick masonry wallettes is shown in Fig. 3. Further details on material properties of masonry can be found in Basha and Kaushik [30]. Compressive strength and stiffness of the fly ash brick masonry was found to be significantly smaller when compared to the commonly used burnt clay brick masonry [31].

In line with the current construction practice in India, three different grades of reinforcing bars were used in the current study (Table 2). In the first stage (Specimens 1–8), the most common reinforcing bars with yield stress f_y as 460 MPa were used as longitudinal bars, and mild steel bars (6 mm diameter) with f_y as 265 MPa were used as shear reinforcement. In the second stage, low strength brittle bars with f_y as 365 MPa were used in specimens 9 and 10 as longitudinal reinforcement, and shear reinforcement consisted of 8 mm diameter bars with f_y as 460 MPa. High strength ductile bars with f_y as 520–530 MPa were used in specimen 11 as both longitudinal and shear (6 mm bars) reinforcement.

In the past studies, a distinction between strong and weak frame with respect to infill strength was not clearly defined. Zovkic et al. [25] and Mehrabi et al. [6] qualitatively reported that strong frames are those designed for seismic actions in which columns and beams had heavier reinforcement near critical regions and expected to behave in ductile mode. Kakaletsis and Karayannis [24], Asteris et al. [32] and Mansouri et al. [33] quantitatively reported frame-infill configuration based on lateral strength of frame and infill, but did not define a range to differentiate the same. Based on these studies, the ratio of frame to infill strength was quantitatively established in the current study. The infill strength (V_{inf}) was calculated as the shear strength of the panel (F_v) times the net-mortared area of the infill (A_n). Lateral Strength of the frame (V_{fr}) was calculated, assuming plastic hinges formed at both ends of the columns, as $4M_p/(h-l_p)$, where M_p is the plastic moment capacity of the column section, h is the height of the column and l_p is the length of plastic hinge (taken as half the depth of the column). The lateral strength of frame and infill was found to be about 40 kN and 23 kN, respectively, and the ratio was about 1.7.

Similarly, ASCE 41 [17] does not explicitly state the type of frame-infill configurations, but defined three ratios of frame to infill strength (<0.7, between 0.7 to 1.3, and $\geqslant$1.3) while defining limits on in-plane lateral drifts. The ratio of frame to infill strength (V_{fr}/V_{inf}) is calculated in ASCE 41 considering the expected story shear strengths of frame (considering bare frame) and infill. The first ratio ($V_{fr}/V_{inf} < 0.7$) corresponds to weak frame-strong infill configuration, and the last ($V_{fr}/V_{inf} \geqslant 1.3$) to strong frame-weak infill configuration. Therefore, considering both qualitative and quantitative estimation, the current system may be termed as strong frame-weak infill configuration (since the ratio is more than 1.3).

4. Testing procedure and instrumentation

The frame specimens were tested under slow-cyclic displacement loading (Fig. 4) applied at the slab level using servo-controlled hydraulic actuator of 250 kN load capacity and a stroke length of ±125 mm (Fig. 1). Experimental results were recorded continuously using load cell and displacement transducer located in the actuator arm, external *LVDT*s (linear varying displacement transducers), and strain gauges. Three cycles of each displacement level were applied and the response was recorded using a data acquisition system. *LVDT*s were used at different locations on the columns and base beam to record the lateral displacements. Base beam was restricted from sliding by bolting it to the strong floor. Quarter-bridge, four wired, linear strain gauges (*HBM* made) were

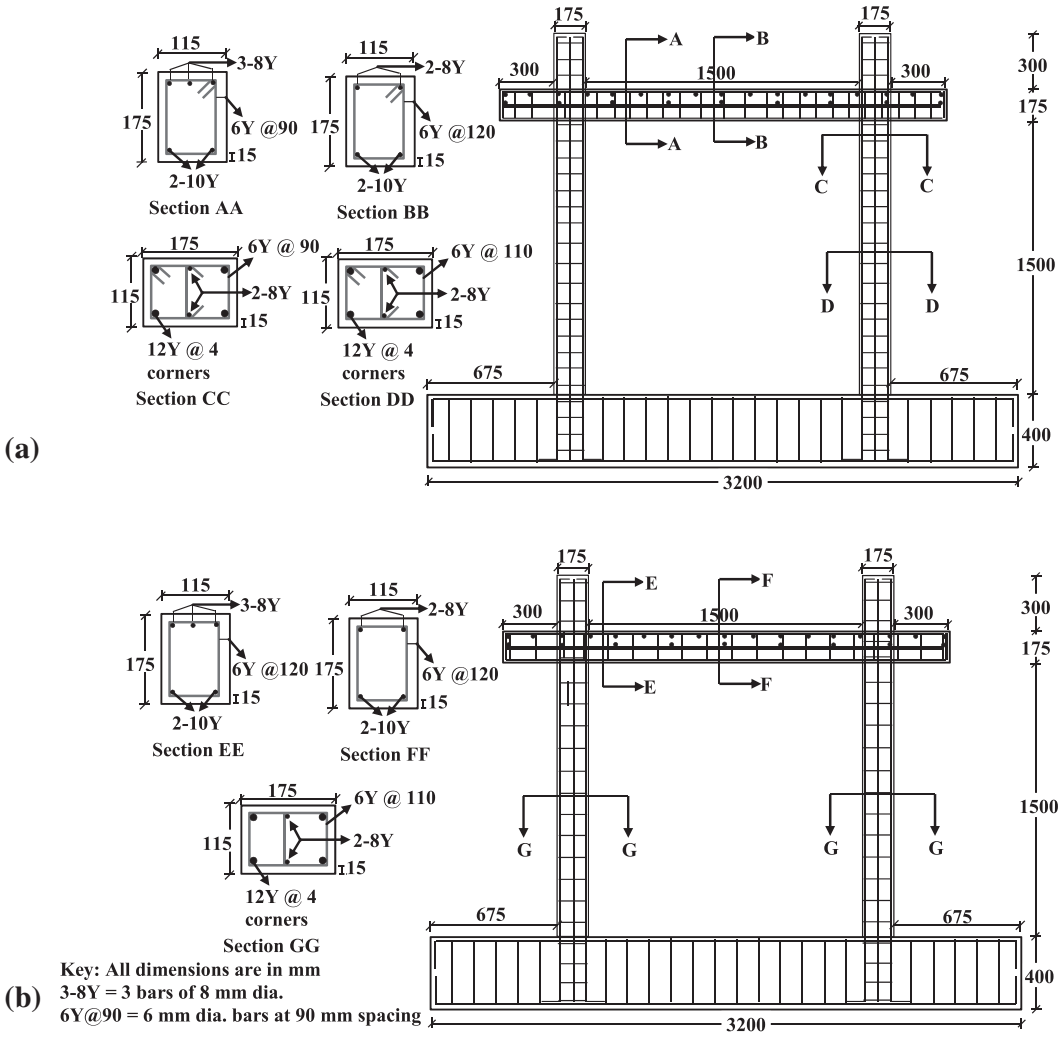

Fig. 2. Reinforcement detailing of: (a) ductile frame; and (b) non-ductile frame model.

Table 2
Material properties of specimens.

Material	Properties	Units	Full-scale bricks	Half-scale bricks
Brick	Dimensions	mm	230 × 110 × 75	110 × 55 × 38
	Compressive strength	MPa	f_b = 5.7, E_b = 3900	f_b = 7.3, E_b = 4960
	Split tensile strength	MPa	f_{bt} = 0.54	f_{bt} = 1.0
Mortar	Compressive strength	MPa	f_j = 17.3, E_j = 7400	f_j = 17.3, E_j = 7400
	Flexural strength	MPa	3.78	3.78
	Split tensile strength	MPa	f_{jt} = 1.2	f_{jt} = 1.2
Masonry prism	Compressive strength	MPa	f'_m = 3.9, E_m = 2700	f'_m = 4.6, E_m = 2800
Masonry wallette	Shear strength	MPa	f'_v = 0.14, G_m = 730	f'_v = 0.14, G_m = 730
Concrete	Compressive strength	MPa	f_{ck} = 22.4, E_c = 23,700	
Longitudinal steel	Tensile strength	MPa	f_y = 460/365/530[a], E_s = 2 × 10^5	
6φ Stirrups	Tensile strength	MPa	f_y = 265/520, E_s = 2 × 10^5	
8φ Stirrups	Tensile strength	MPa	f_y = 460, E_s = 2 × 10^5	

[a] Three types of reinforcing bars were used.

used to record the strains in the reinforcement. Strain gauges were bonded to the longitudinal reinforcement at the most likely locations of formation of plastic hinges from the face of beam and columns (Fig. 1). Maximum lateral load resistance of the specimens is reported in both push (−) and pull (+) directions. In the current study, tests were terminated when the capacity of the specimen reduced to about 75% of its maximum or when the failure was imminent.

5. Hysteretic response of specimens

The lateral load behavior of specimens during slow cyclic loading in the form of hysteretic response (actuator load-lateral deformation) for first cycle of every lateral displacement level is shown in Fig. 5. In ductile and non-ductile bare frames, hysteretic loops were evenly spaced before and after reaching the lateral load capacity. The non-ductile bare frame exhibited higher amount of

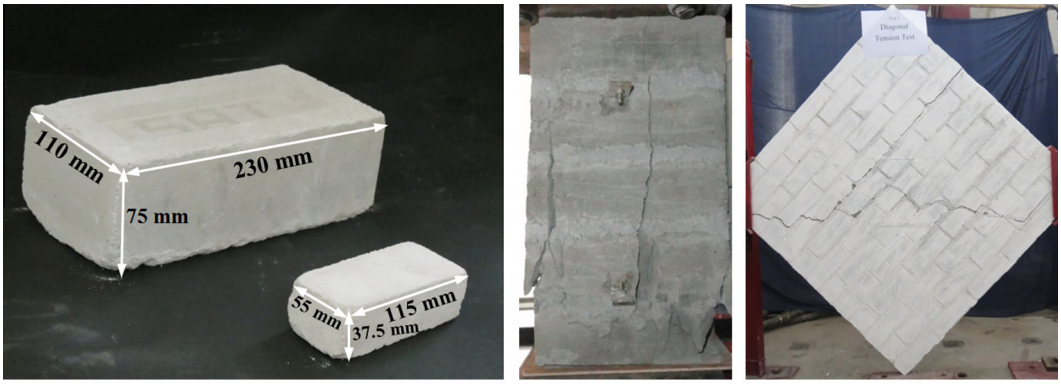

Fig. 3. (a) Description of full-scale and half-scale bricks; failure of: (b) masonry prism; and (c) masonry wallette.

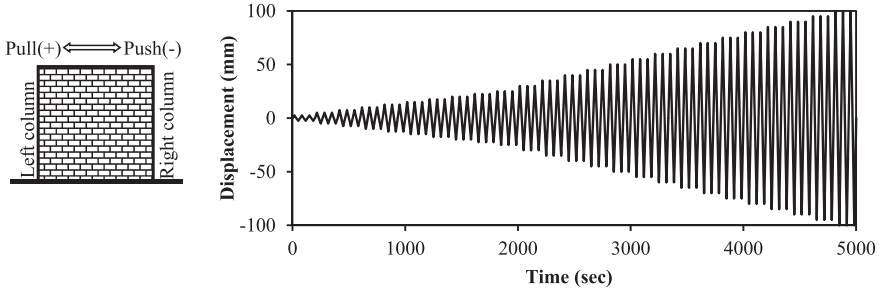

Fig. 4. Push and pull directions and displacement cycles of the actuator for slow cyclic test.

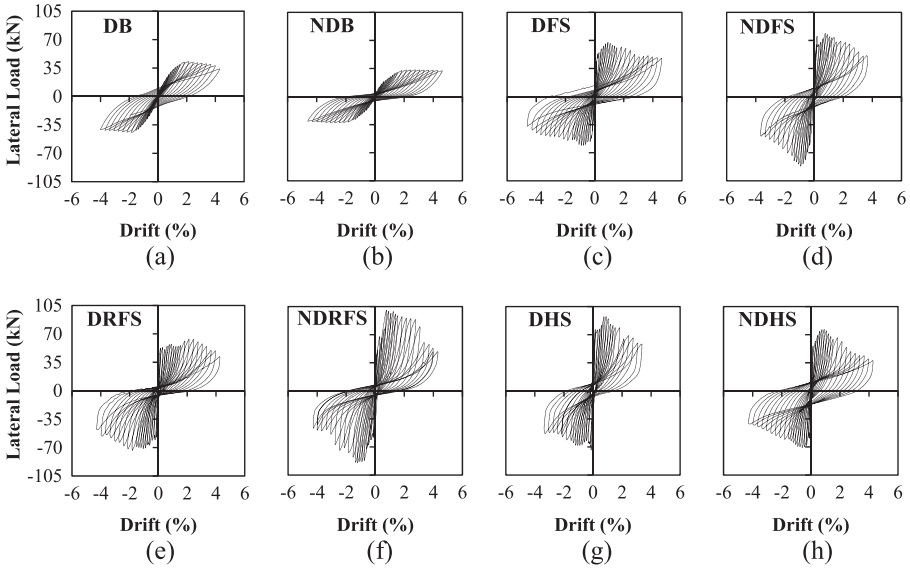

Fig. 5. Hysteretic response of specimens 1–8: (a) ductile bare frame; (b) non-ductile bare frame; (c) ductile frame infilled with full-scale bricks; (d) non-ductile frame infilled with full-scale bricks; (e) ductile retrofitted frame infilled with full-scale bricks; (f) non-ductile retrofitted frame infilled with full-scale bricks; (g) ductile frame infilled with half-scale bricks; and (h) non-ductile frame infilled with half-scale bricks. (*Key:* D – Ductile; ND – Non ductile; B – Bare; FS – Full-scale bricks; HS – Half-scale bricks; R – Retrofitted.)

pinching when compared to the ductile frame, and therefore, dissipated lesser amount of energy. In case of infilled frames, initially the loops were closely spaced until the lateral load carrying capacity was reached.

As the infill wall cracked and gaps developed along the frame-infill interface, hysteretic loops were found to be unevenly spaced (i.e., slight uneven variation in the lateral load resistance and pinching was observed due to reorganization of infill after infill failure). Pinching in hysteresis loops of infilled frames (Specimens 3–8) was more pronouncing at higher displacement levels. This shows that the resistance provided by the infill decreased after significant damage in the infill. The beneficial effect of ductile detailing was evident in infilled frames only after the frame reached its maximum capacity. The dropdown in load carrying capacity was

gradual in case of ductile infilled frames when compared to corresponding non-ductile frames (full- or half-scale bricks).

6. Evaluation of influencing parameters

The parameters influencing the behavior of test specimens were quantified in terms of lateral strength, lateral stiffness, and energy dissipation. Initial stiffness was calculated as the slope of the secant connecting 5–33% of the lateral load corresponding to the first hysteretic loop (first displacement level). It was observed that initial stiffness of the infilled frames was about 7–10 times that of the corresponding bare frames (Fig. 6(a) and Table 3). Frames infilled with half-scale bricks observed marginally higher initial stiffness (3% for non-ductile and 8% for ductile) when compared to frames infilled with full-scale bricks. The reason for the frames to observe slightly higher initial stiffness may be due to the fact that the frames resisted slightly higher lateral load in the initial drift level (0.15%). English bond used in case of half-scale brick specimens appears to have provided higher lateral load resistance in the initial drift level when compared to lateral load resistance provided by the stretcher (running) bond in case of full-scale brick specimens.

The lateral strength of frames infilled with full-scale bricks was about 1.6 (ductile) and 2.5 (non-ductile) times that of their corresponding bare frames. Frames infilled with half-scale bricks resisted a lateral strength of about 1.9 (ductile) and 2.2 (non-ductile) times that of the corresponding bare frames. As discussed earlier, the difference in the brick bond pattern possibly resulted in slightly higher lateral strength of frames infilled with half-scale bricks compared to frames infilled with full-scale bricks. The crack propagation in infill in case of full-scale bricks was easier as the bricks were laid in stretcher (running) bond, whereas, in the case of half-scale bricks the crack propagation was difficult due to the presence of alternate courses of headers and stretchers. Further, Chiou and Hwang [34] reported that the compressive strength of mortar is also one of the factors that influence the lateral strength of the infilled frames. Mortar used in the current study was stronger and stiffer than the bricks (Table 2), and the number of mortar layers provided in half-scale brick specimens (Specimens 7 and 8) was higher (almost double). Further, compressive and tensile strength of half-scale bricks and masonry prism strength for half-scale specimens is higher than that of the full-scale brick specimens. These factors further resulted in higher lateral load resistance of the half-scale brick specimens. The lateral strength of retrofitted frames was approximately equal to that of the original infilled frames (Specimens 4 and 5), highlighting the effectiveness of the retrofitting technique in restoring the original capacity of the structure.

Energy dissipation per displacement level was computed as the area enclosed under the hysteresis loops (3 loops per displacement level), and the cumulative energy dissipation is calculated by summing the individual areas of each displacement level (Table 3). Energy dissipation during the initial stages was due to the contribution of frame and infill. After significant damage in infill, dissipation was primarily due to the formation of plastic hinges in columns of the frame. Energy dissipation can be quantified based on the lateral strength, displacement sustained, and the effect of pinching as described earlier. The amount of energy dissipated by the frames infilled with full-scale bricks was about 1.5 (ductile) and 1.6 (non-ductile) times that of the corresponding bare frames (Fig. 6(b) and Table 3). As expected, the energy dissipated by the ductile frame infilled with full-scale bricks was higher (about 20% more) when compared to the non-ductile frame. This is because in ductile frame, the degradation of strength was gradual, ultimate displacement levels were larger (75 mm), and lesser pinching was observed in hysteretic behavior (Fig. 5). Frames infilled with half-scale bricks showed an energy dissipation of about the same (in case of ductile frame) and about 2.3 times (in case of non-ductile frame) that of their respective bare frames. Non-ductile frame infilled with half-scale bricks dissipated highest energy due to the lesser amount of pinching (Fig. 5(h)).

Compared to other infilled frames, non-ductile frame infilled with half-scale bricks (Specimen 8) developed high friction mechanism between brick layers due to intense sliding cracks along bed and head mortar joints, and vertical splitting cracks in bricks. However, in case of ductile frame infilled with half-scale bricks (Specimen 7) only bed joint sliding of brick layers and minimal vertical splitting cracks in bricks was observed (Fig. 7(g) and (h)). Under lateral loading, more cracks were formed in infill in non-ductile half-scale specimen due to more number of mortar joints in alternate courses of headers and stretchers, and it was also observed that cracking in infill in case of ductile frame infilled with half-scale bricks was limited to a few brick layers. Stylianidis [35] reported that at higher drift levels the contribution of infill to energy dissipation was negligible as infill degrades rapidly. On the contrary, in non-ductile frame infilled with half-scale bricks, infill was found to remain intact with the bounding frame even

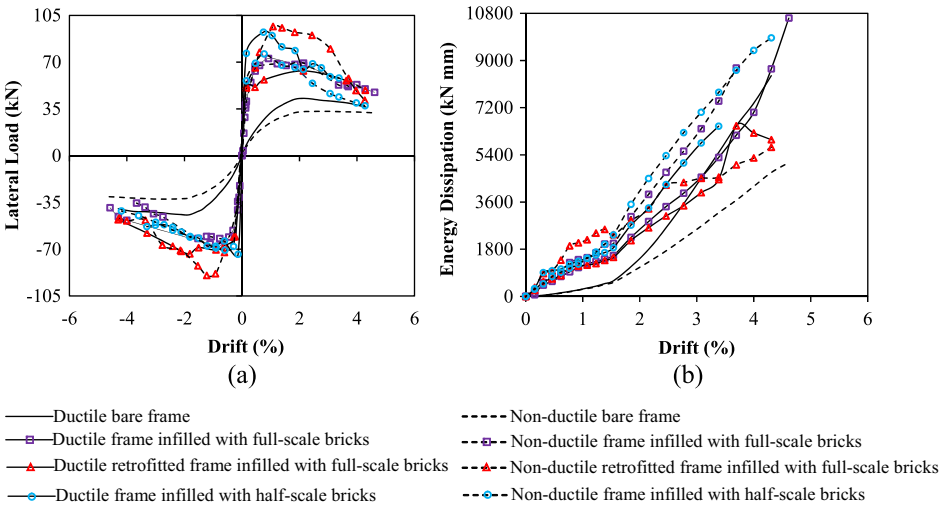

Fig. 6. Lateral load behavior of specimens (1–8): (a) envelope curves showing force vs. displacement at actuator level; (b) energy dissipation at different displacement levels.

Table 3
Influencing parameters of tested specimens.

Specimen no.	Type of frame	K_i (kN/mm)	ED (kNmm)	F (kN)	δ_u (mm)	DR_i	DR_f	DR_s	DR_{80}	DR_u
						(%)				
1	Ductile bare frame	4.0	43,900	−44, +43	70	–	0.62	1.38	–	4.31
2	Non-ductile bare frame	3.2	32,100	−33, +33	75	–	0.46	0.77	–	4.62
3	Ductile frame infilled with full-scale bricks	28.6	64,300	−68, +73	75	0.31	0.77	0.77	−3.3, +2.9	4.62
4	Non-ductile frame infilled with full-scale bricks	29.2	51,900	−87, +79	60	0.31	1.08	0.46	−1.9, +2.6	3.69
5	Ductile retrofitted frame infilled with full-scale bricks	30.5	48,300	−73, +63	70	0.15	0.92	0.46	−3.2, +3.8	4.31
6	Non-ductile retrofitted frame infilled with full-scale bricks	31.2	56,900	−90, +101	70	0.15	0.77	0.62	−2.6, +3.1	4.31
7	Ductile frame infilled with half-scale bricks	31.0	40,200	−74, +93	55	0.15	1.23	0.46	−1.9, +1.9	3.38
8	Non-ductile frame infilled with half-scale bricks	30.1	74,500	−71, +76	70	0.15	0.77	0.62	−2.2, +2.1	4.31
9	Ductile infilled frame with improved shear capacity throughout the length of the column	30.3	64,300	−46, +55	80	0.31	0.92	0.92	−2.6, +3.8	4.92
10	Ductile infilled frame with improved shear capacity in critical regions only	30.5	62,400	−45, +60	80	0.31	0.77	0.92	−3.6, +3.9	4.92
11	Ductile infilled frame with improved shear capacity in critical regions using high strength bars	35.7	78,200	−105, +107	95	0.46	0.92	0.77	−2.7, +2.0	5.85

Note: K_i is the initial stiffness, ED is the cumulative energy dissipation, F is the maximum lateral load, δ_u is the ultimate lateral displacement, DR_i, DR_f, DR_s, DR_{80}, and DR_u represents the drift at initiation of crack in infill (sliding/diagonal), initiation of flexural cracks in columns, initiation of shear cracks in columns, 80% of maximum load, and ultimate deformation, respectively.

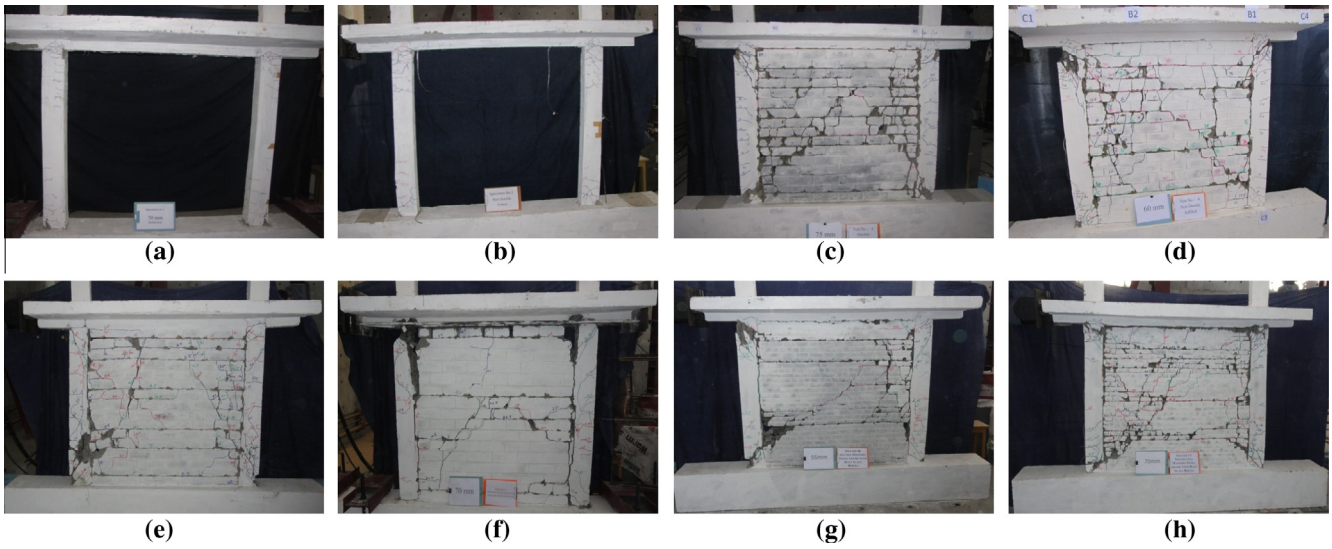

Fig. 7. Failure mechanisms observed in specimens 1–8: (a) ductile bare frame; (b) non-ductile bare frame; (c) ductile frame infilled with full-scale bricks; (d) non-ductile frame infilled with full-scale bricks; (e) ductile retrofitted frame infilled with full-scale bricks; (f) non-ductile retrofitted frame infilled with full-scale bricks; (g) ductile frame infilled with half-scale bricks; (h) non-ductile frame infilled with half-scale bricks.

at higher drift levels, and therefore, contributed to higher energy dissipation due to the friction mechanism as compared to other infilled frames (Specimen 3–7). Energy dissipated by the retrofitted frames was about 0.8 (ductile) and 1.1 (non-ductile) times that of the original specimens (3 and 4). This is due to the fact that the ductile retrofitted frame (Specimen 5) underwent lesser ultimate lateral displacement and higher pinching when compared to other infilled frames.

Drift ratio (ratio of lateral displacement to storey height) was calculated corresponding to major events such as formation of infill cracks (sliding and diagonal cracking), initiation of shear cracks and flexure cracks in columns, peak load and 80% of peak load in post peak regime. Slight variations in quantification of influencing parameters is expected due to poor quality of bricks available in the region, variable workmanship, variable thickness of mortar joints, and improper bond and interface connections between infill and frame. From the current study, it may be inferred that since the masonry infilled RC frames are quite stiffer systems than the bare frames, it may not be practical to compare the lateral strength and stiffness of ductile and non-ductile specimens because the initial behavior depends primarily on the infill properties.

7. Crack patterns and failure mechanisms

Crack patterns observed in various members provide an insight into the lateral load resistance path, damage pattern, and mode of failure, which depends on the relative strength of frame and infill. The crack pattern observed in all the specimens and resulting failure mechanisms are discussed below.

7.1. Ductile and non-ductile bare frame (Specimens 1 and 2)

The crack pattern observed in both ductile and non-ductile bare frames was similar, but the amount of cracks developed in

non-ductile frame was higher in which cracks initiated at 0.46% drift (lateral load of 15 kN). In ductile bare frame, flexural cracks initiated at a drift of 0.62% and lateral load of 24 kN near left beam–column joint (Fig. 7(a) and (b)). With increase in lateral drift, minor diagonal shear cracks developed in non-ductile columns at a drift of 0.77% (21 kN), whereas, in ductile columns shear cracks developed at 1.38% drift (40 kN). Few cracks were observed in beams in both the bare frames emphasizing the T-beam action due to the presence of RC slab. Finally, it was ascertained that though significant shear cracks developed in columns of non-ductile frame, both ductile and non-ductile bare frames failed due to flexural mechanism in columns.

7.2. Ductile and non-ductile infilled frames (Specimens 3–8)

In case of infilled frames, both ductile and non-ductile, cracks formed initially in infill, and with increasing lateral drift, cracks propagated into frame members. The drift levels corresponding to the initiation of major events in infilled frames are shown in Table 3. It was observed that the initiation of cracks in frame elements depends on the location of cracks in infills. Cracks in infill panels originated mainly from two locations: one near the mid-height of the infill panel and the other slightly below the soffit of the top beam or slightly above the bottom beam. Specimens 3, 6, and 8 observed bed joint sliding cracks in infill near mid-height at a drift level of 0.31% (56 kN), 0.15% (57 kN), and 0.15% (59 kN), respectively. In case of ductile frame infilled with full-scale bricks (Specimen 3), bed joint sliding cracks near the mid-height of the panel were connected by diagonal stepped cracks (cracks in both bed and mortar head joints and vertical splitting cracks in bricks) originated from the column ends. Later the cracks propagated to the opposite column ends by similar diagonal stepped cracks. Whereas, in case of specimens 6 and 8, the bed joint sliding cracks in the middle of the panel were connected by vertical interface cracking between infill and column in upper middle panel and propagated to the opposite ends by diagonal stepped cracking in the lower middle infill panel.

On the other hand, in specimens 4, 5, and 7 bed joint sliding cracks formed slightly away from the mid-height of the infill panel (i.e., below top beam soffit and above the bottom beam) at a drift level of 0.31% (−61 kN, 75 kN), 0.15% (57 kN), and 0.15% (77 kN), respectively. In case of specimen 4, cracks in infill commenced at a drift level of 0.31% (−61 kN, +75 kN), 3 courses above and below the mid-height of the panel and later these bed joint sliding cracks were joined by diagonal stepped cracks. Bed joint sliding cracks in ductile retrofitted frame (Specimen 5) were initiated away from the mid-height of the infill panel at 0.15% (57 kN) drift level two courses below the soffit of the beam. Similar sliding cracks were formed away from mid height of the panel four courses above the bottom beam at next drift level of 0.32% (60 kN), with vertical cracks along the column-wall interface. In case of specimen 7, bed joint sliding cracks in infill initiated four courses below the soffit of the top beam at a lateral load of 77 kN (0.15% drift). Later similar cracks were formed nine courses above the top of the bottom beam away from the mid-height of the infill panel in the subsequent 0.31% drift (−66 kN, +76 kN) in addition to cracks along the column-wall interface (Fig. 7(g)).

Formation of bed joint sliding cracks away from the mid-height weakened the interface connection between infill and column, and decreased the effective length of column in contact with infill (thus creating captive column effect). This resulted in concentration of the entire inter-story drift within the column free length, thereby increasing the chord rotation demand at both ends of the columns. Since the shear span (moment to shear ratio) for captive columns is short, diagonal shear cracks (diagonal tensile cracks) developed/initiated along the free length of the columns at a smaller drift level. Similar behavior of masonry infilled RC frames is also reported in past literature [9]. Due to the formation of bed joint sliding cracks away from the mid-height of infill panel in specimens 4, 5, and 7, diagonal shear cracks initiated in columns at a smaller drift level of 0.46% (69 kN), 0.46% (61 kN), and 0.46% (77 kN). With increase in drift levels, bed joint sliding cracks in specimens 3, 6, and 8 also started forming away from the mid-height of the panel leading to diagonal shear cracks (diagonal tensile cracks) at a drift level of 0.77% (70 kN), 0.62% (77 kN), and 0.62% (74 kN), respectively. Interestingly, the first crack formed in columns was diagonal shear crack (diagonal tensile cracks) in most of the infilled specimens.

As the drift levels increased, flexural cracks initiated along the length of the columns. In specimens 3, 6, and 8 flexural cracks initiated almost simultaneously along with diagonal shear cracks (Table 3), whereas the flexural cracks in specimens 4, 5, and 7 were delayed as most of the cracks formed in infill. In all the infilled frame specimens, very few cracks formed in the beams due to the strong T-beam action provided by the slab. Subsequent widening of shear cracks, spalling of cover concrete and buckling of longitudinal reinforcement was observed in case of ductile frames infilled with full-scale and half-scale bricks (Specimens 3 and 7). In case of non-ductile infilled frames, opening of 90° hook along with widening of shear cracks and buckling of longitudinal reinforcement was observed. Damage to infills in both the retrofitted frames (Specimens 5 and 6) was lesser compared to the original frames (Specimens 3 and 4).

From the available strain gauge data, photographic study, and from visual inspection, it was observed that the shear cracks in the columns were formed much earlier than the first yielding of the column reinforcing bars. Further, widening (opening) of shear cracks in columns also occurred before the yielding/buckling of reinforcing bars in columns. In specimen 3 (ductile frame), widening of shear cracks and subsequent spalling of concrete was observed at a drift level of 4.3% followed by buckling of longitudinal reinforcement near the column ends at a drift level of 4.62%. Whereas, specimen 4 (non-ductile frame) observed widening of diagonal shear cracks at a lower drift level (2.46%) with subsequent buckling of longitudinal reinforcement at 3.38% drift level. In case of retrofitted frames, widening of shear cracks was observed at a drift level of 3.38% and 2.15% for specimens 5 and 6, respectively. From the analysis of strain data, it was observed that yielding/buckling of longitudinal reinforcement occurred at 4% (Specimen 5) and 2.76% drift level (Specimen 6). Specimens 7 and 8 observed widening of shear cracks at 2.76% and 2.46% drift, respectively, and yielding/buckling of longitudinal reinforcement at about 3.38% drift level.

The tests were terminated when the capacity of the specimen reduced to about 75% of its maximum or when the failure was evident. Most of the cracks developed near the column ends in infilled frames were primarily diagonal in nature (45° to the direction of loading) due to the diagonal strut effect of infill along the contact length of column. With increase in drift level, widening of the diagonal shear cracks followed by spalling of concrete between the widened cracks was observed. This resulted in opening of hooks of shear reinforcement followed by yielding/buckling of longitudinal reinforcement in the spalled concrete region. A few flexural cracks were also formed in the columns of some specimens parallel to the direction of loading; these cracks propagated towards the shear cracks with increasing drift. This observed behavior of infilled frames was completely different than the bare frame, which exhibited flexural mode of failure. Based on these observations, the failure mechanism in case of infilled frames was termed as shear failure of columns. Similar failure mechanisms were also reported in the past experimental studies [6–8,32]. The test was terminated at a drift level of 4.62% (−39 kN, 47 kN) and 3.69% (−35 kN, 52 kN)

in ductile and non-ductile infilled frames (Specimens 3 and 4), respectively, when crushing or spalling of concrete along the diagonal shear cracks and buckling of longitudinal reinforcement was observed in both the columns (Fig. 7(c) and (d)). In case of retrofitted frames (specimens 5 and 6), the tests were terminated when both the columns failed in shear and crushing or spalling of concrete between the widened shear cracks was observed at lateral drift level of 4.31% and lateral load level 48 kN for both specimens (Fig. 7(e) and (f)). Specimens 7 and 8 with half-scale bricks were tested till a drift level of 3.38% (58 kN), and 4.31% (41 kN), respectively, when shear failure in column and out-of-plane movement of infill wall was observed (Fig. 7(g) and (h)).

In the current study, frames with a moderately higher aspect ratio ($h/l \sim 1$) were tested, and it was observed that all the infilled frames failed due to shear failure of columns. Therefore, it becomes important to find out methods for improvement of lateral load behavior of masonry infilled RC frames such that shear failure of columns can be prevented.

8. Improving shear capacity of masonry infilled RC frames

The frames considered in the current study were designed to exhibit flexural behavior. However, columns of the frames failed in shear failure mode when infill walls were introduced. This is primarily due to excessive shear demand on columns from infills for which the columns were not designed. Past literature [6,15,36] reported that columns do not fail in shear in case of strong frame-weak infill configuration. But in the current study, though strong frame-weak infill configuration was used, all the columns of infilled frames failed in shear mode irrespective of the reinforcement detailing in RC members (ductile or non-ductile) and size of bricks used (full-scale or half-scale).

In order to prevent/delay the shear failure in columns, shear design of columns was upgraded following the guidelines of Eurocode 8 [16], ASCE 41 [17], and IS 13920 [28]. IS 13920 recommends special confining reinforcement in columns, only if significant variation in stiffness is observed along the column length. Area of shear reinforcement required as special confining reinforcement (A_{sh}) can be calculated using Eq. (1).

$$A_{sh} = 0.18sh\frac{f_{ck}}{f_y}\left(\frac{A_g}{A_k} - 1\right) \quad \text{(All units in N, mm)} \tag{1}$$

A_{sh} is the area of the bar, s is the spacing of hoops, h is the longer dimension of the rectangular confining core measured to its outer face, A_g is the gross area of the column cross section, and A_k is the area of the confined core in the rectangular hoop measured to its outside dimensions. In the current study, special confining reinforcement in critical regions works out to be 3 legged, 8 mm diameter bars at a spacing of 90 mm. With this shear reinforcement, the shear capacity of the column in critical region comes out to be 135 kN using the method prescribed in the code [28].

Similarly, according to Eurocode 8, the amount of transverse reinforcement required to be provided in critical regions should satisfy Eq. (2), especially at column base.

$$\alpha\omega_{wd} \geqslant 30\mu_\varphi \nu_d \varepsilon_{sy,d}\frac{b_c}{b_0} - 0.035 \tag{2}$$

α is confinement effectiveness factor ($=\alpha_n\alpha_s$), ω_{wd} is mechanical volumetric ratio of confining hoops within the critical regions, μ_φ is curvature ductility factor, ν_d is normalized design axial force, $\varepsilon_{sy,d}$ is design value of the tension steel strain at yield, b_c and b_o represent the width of gross cross section and confined core, respectively, $\alpha_n = 1 - \sum_n b_i^2/6b_0h_0$, $\alpha_s = (1 - s/2b_0)(1 - s/2h_0)$, n is number of longitudinal bars laterally engaged by hoops or cross ties, s is the spacing of the transverse reinforcement, b_i is the distance between the consecutive engaged bars, and h_0 is the depth of the confined core. The required volumetric ratio (ω_{wd}) works out to be about 0.65 in the present study, whereas, in case of special confining reinforcement using Eq. (1), it was found to be 0.71.

Eurocode 8 also recommends verifying the shear capacity in column length over which diagonal strut force is applied for the smaller of the two shear forces (V_d): (a) horizontal component of the strut force of infill, taken equal to the horizontal shear strength of the panel which is calculated using Eq. (3); and (b) the shear force computed in accordance with Eq. (4), considering the clear length of column equal to the contact length (l_c) of the infill.

$$V_d = f'_v A_n \tag{3}$$

$$V_d = \gamma_{Rd,c}\left(\frac{2M_{Rd,c}}{l_c}\right) \tag{4}$$

where f'_v represent the shear strength of the wall, A_n represent the net mortared area, which is equal to infill wall thickness (110 mm) times the clear length of the infill wall (1500 mm), $\gamma_{Rd,c}$ is the overstrength factor due to steel hardening (=1.3 for high ductility class *DCH*), $M_{Rd,c}$ represents the design flexural capacity of the column, and l_c is the contact length of the column equal to the full vertical width of the diagonal strut of the infill. Contact length of infill was calculated as width of the strut times Cosine of angle θ, which is taken as the ratio of height of the infill (1500 mm) to length of the infill (1500 mm). The shear strength of the panel was taken as diagonal tension strength of the infill wall as reported by Dizhur and Ingham [37]. The shear strength of the panel was about 0.14 MPa (Table 2) and the horizontal component of the strut force was calculated using Eq. (3) is 23 kN. The shear force computed using Eq. (4) was found to be 121 kN considering the width of the strut equal to one tenth of the diagonal length of the infill wall obtained using past literature [17,19,38].

Similarly, ASCE 41 [17] recommends checking the shear strength of the column members adjacent to the infill panels for higher of: (a) horizontal component of the strut force at the column using the shear strength of the column with zero axial load; and (b) the shear force obtained from development of column flexural strengths at top and bottom. These two recommendations of ASCE 41 are in line with the recommendations of Eurocode 8; out of the two, the second dominates. Since IS 13920 requirements were found to be more stringent, columns were provided with 3 legged stirrups of 8 mm diameter bars at 90 mm spacing. Both IS 13920 and Eurocode 8 recommend the length of critical region (from the face of the joint), in which closely spaced shear reinforcement is required to be provided, as larger of: largest dimension of member, 1/6 of the clear span, and 450 mm. In the current study, the critical length comes out to be 450 mm.

To verify the effectiveness of these design provisions in earthquake standards in preventing/delaying shear failure in RC columns of infilled frames, three ductile frames infilled with full-scale bricks with different shear reinforcement in columns were tested in the second stage. In the first infilled frame with improved shear capacity throughout the length of the column (Specimen 9), 8 mm diameter bars (f_y = 460 MPa) with 3-legged stirrups were provided at 90 mm spacing throughout the length of the column. In the second infilled frame with improved shear capacity in critical regions only (Specimen 10), 8 mm diameter bars (f_y = 460 MPa), 3-legged stirrups were provided at 90 mm spacing only in critical regions (about 500 mm from the face of top and bottom beam), and a spacing of 110 mm was maintained in the remaining length. In case of specimen 11, high strength deformed bars were used in both longitudinal (f_y = 530 MPa) and transverse reinforcement (f_y = 520 MPa). The shear reinforcement consisted of 3-legged, 6 mm diameter bars at a spacing of 90 mm in critical regions only.

8.1. Lateral load response of frames with improved shear capacity (Specimens 9–11)

In the second stage, slow cyclic lateral load tests were carried out on three specimens in which shear capacity of columns was enhanced and the results are reported in Table 3 and Fig. 8. It can be observed that the hysteresis loops were closely spaced in the initial displacement cycles until infill reached its capacity, and later the loops were unevenly spaced as observed in the previous specimens. Fig. 9 compares the lateral load–displacement envelope and energy dissipation curves obtained for frames infilled with improved shear capacity with that obtained for original infilled frames. Though the initial stiffness of frames with improved shear capacity throughout length of the column and in critical regions was similar to that of the original infilled frame specimens (Table 3), ductile frame with improved shear capacity using high strength bars exhibited about 15% more lateral stiffness. Lateral load carrying capacity of shear capacity improved frames (Specimens 9 and 10) was slightly lower than that of ductile frame infilled with full-scale bricks due to the use of weaker and brittle reinforcing bars. Degradation of lateral load carrying capacity was found to be gradual in case of improved frames (Specimens 9 and 10), whereas, sudden dropdown was observed in case of previously tested infilled frame specimens (Fig. 6(a)).

Frame with improved shear capacity using high strength bars (Specimen 11) exhibited highest lateral load carrying capacity (about 1.5 times that of original ductile infilled frame) at a very low drift level (0.46%). Nevertheless, the subsequent sudden dropdown was observed in strength similar to that observed in the original infilled frame specimens (Specimens 3 and 4). Energy dissipated by frame with improved shear capacity throughout the length of the column and in critical regions was similar to that dissipated by the previously tested infilled frames (Table 3 and Fig. 9(b)), whereas, energy dissipation by frame with improved shear capacity using high strength bars was significantly higher. Experimental results showed that using special confining reinforcement is beneficial in enhancing the lateral load behavior of infilled frames, especially in improving the post-peak load behavior, energy dissipation, and ultimate deformation capacity. Effectiveness of using regular and spiral rectangular shear reinforcement in columns of one third-scale infilled RC frames was investigated by Kakaletsis et al. [36] under two cycles of reversible loading. It was reported that the average lateral strength and energy dissipation of the weak infilled frame was about 1.84 and 1.64 times that of the bare frame, respectively. In the current study, the lateral load carrying capacity and energy dissipation capacity of the improved frames was found to be about 1.2–2.4 and 1.42–1.78 times that of the bare frame, respectively, for three cycles of lateral loading.

As observed in original infilled frame specimens (Specimens 3 and 4), first major crack in case of frames with improved shear capacity throughout the length of the column and in critical regions only (Specimens 9 and 10) was observed along the column-wall interface and bed joints at a drift level of 0.31% (51 kN) (Fig. 10). In case of frame with improved shear capacity in critical regions using high strength bars (Specimen 11), cracks appeared in infill as diagonal stepped cracks with bed joint sliding cracks near the mid-height of infill panel at a drift level of 0.46% (107 kN). Till 0.62% drift level most of the cracks were concentrated in infill. At a drift level of 0.77%, flexural cracks along the length of the column and diagonal shear cracks near the ends of columns developed in specimens 10 and 11, respectively, whereas in case of frame with improved shear capacity throughout the length of column (Specimen 9), flexural cracks and diagonal shear cracks in columns developed at a higher drift 0.92% (54 kN). Interestingly, shear cracks initiated at a lower drift level of 0.46% (Specimens 4, 5, 7) to 0.77% (Specimen 3) in original ductile and non-ductile infilled frame specimens (Table 3). Therefore, providing special confining reinforcement in columns may help in delaying the initiation of shear cracks in columns. With increase in drift level, further sliding of brick layers and formation of flexural cracks along the length of the columns was observed.

The frame with improved shear capacity using high strength deformed bars (Specimen 11) enhanced the lateral load carrying capacity and stiffness but the amount of shear cracks in columns was significantly more compared to specimens 9 and 10. Clearly, use of lower yield strength reinforcing bars in columns did not result in improved performance due to buckling of longitudinal reinforcement. But even before buckling of longitudinal steel in column, significant damage occurred in column due to the formation of shear cracks. In case of specimens 9, 10, and 11 widening of shear cracks was observed at a drift level of 4%, 3.69%, and 2.46%, respectively. Subsequently, spalling or crushing of concrete was observed between the widened shear cracks at a drift level of 4.6%, 4.3%, and 3.69% respectively. The tests were terminated when out-of-plane fall out of infill, buckling of longitudinal reinforcement was observed in the spalled concrete region at a drift level of 4.92% (Specimens 9 and 10) and 5.85% (Specimen 11). Fig. 10 represent the failure pattern observed at the termination of tests, where it appears that failure was by flexural hinging in columns near the column ends, but it was observed during testing, that spalling of concrete and buckling of reinforcement occurred due to the widening of shear cracks. Therefore, the failure mode was termed as shear failure in columns. Though infilled frames with improved shear capacity showed better behavior compared to all other infilled frames in terms of delaying shear failure, it fell short of expectations, as the desired behavior (flexural failure of columns instead of shear failure) could not be achieved.

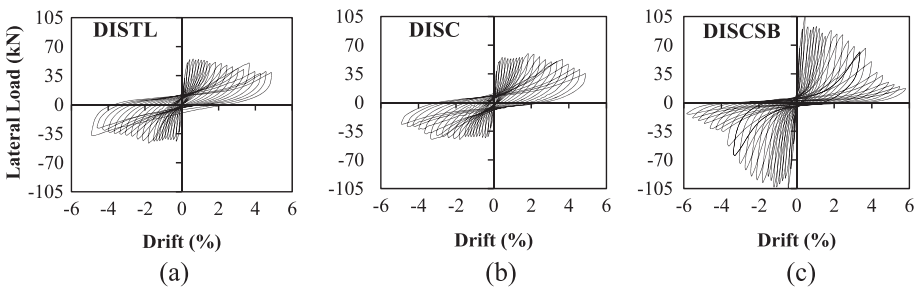

Fig. 8. Hysteretic response of specimens 9–11: (a) ductile infilled frame with improved shear capacity throughout the length of column; (b) ductile infilled frame with improved shear capacity in critical regions only; (c) ductile infilled frame with improved shear capacity in critical regions using high strength bars. (*Key:* D – Ductile; I – Improved; S – Shear capacity; TL – Throughout Length; C – Critical regions; SB – High strength bars.)

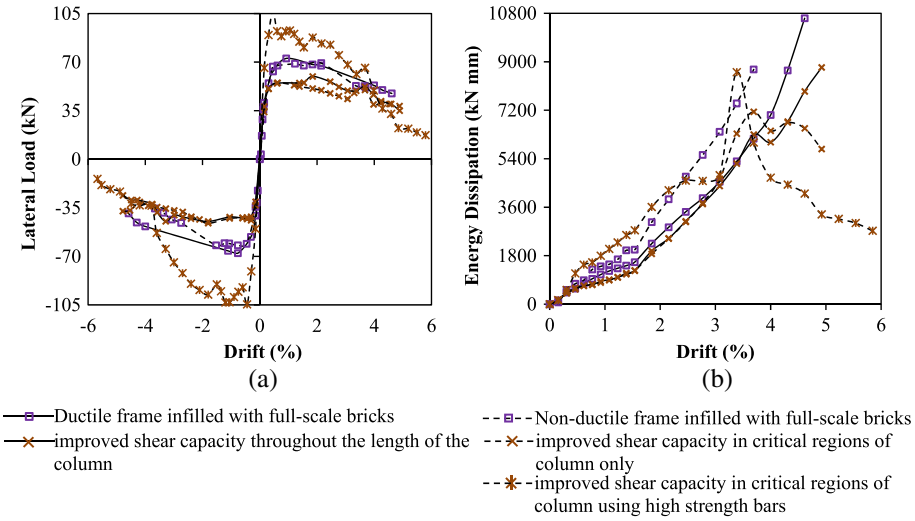

Fig. 9. Comparison of lateral load behavior of specimens 3, 4, 9, 10 and 11: (a) envelope curves showing force vs. displacement at actuator level; and (b) energy dissipation at different displacement levels.

Fig. 10. Failure mechanisms observed in specimens 9–11: (a) ductile infilled frame with improved shear capacity throughout the length of column; (b) ductile infilled frame with improved shear capacity in critical regions; (c) ductile infilled frame with improved shear capacity in critical regions using high strength bars.

9. Idealization of load–displacement relationship for infilled frames

The drift levels corresponding to onset of major damage in masonry infilled RC frames, as also discussed by other investigators [6,7], can serve as a guideline for design of similar infilled frames for a particular performance level. Using the lateral drift levels obtained in the current study (Table 3), an idealized load–displacement relationship is proposed (Fig. 11) by considering the average points corresponding to the onset of major events (infill cracks, shear cracks, flexure cracks, peak load, and 80% post peak load).

The lateral load on primary *y*-axis of Fig. 11 is normalized with the average lateral load carrying capacity, and the secondary *y*-axis shows the base shear ratio (lateral load normalized with seismic weight). Large deviations in a set of values is not considered while averaging particular set of data and the considered values are clubbed into a set of packets (dotted line boxes in Fig. 11). The first major event observed was initiation of cracks (diagonal and sliding) in infill. Infilled frames behaved linearly till an average drift level of 0.23% [coefficient of variation, *COV* 0.36] corresponding to a load level of about 78% of lateral load capacity [*COV* 0.17]. Similarly, Mehrabi et al. [6] tested half-scale RC frames infilled with strong and weak masonry under monotonic and cyclic loading and defined serviceability limit state as the drift corresponding to the initiation of damage in infills. Subsequently, RC columns start behaving non-linearly as shear cracks and flexural cracks are initiated at a drift level of 0.58% [*COV* 0.22] and 0.88% [*COV* 0.17], respectively, corresponding to a lateral load of about 95% [*COV* 0.05] and 100% [*COV* 0.09], respectively, of the peak load. It can be observed that lateral strength of most of the specimens reached at a drift level corresponding to the initiation of flexure cracks in columns. The post-peak drift corresponding to 80% [*COV* 0.14] of the lateral strength of the infilled frame was in the range

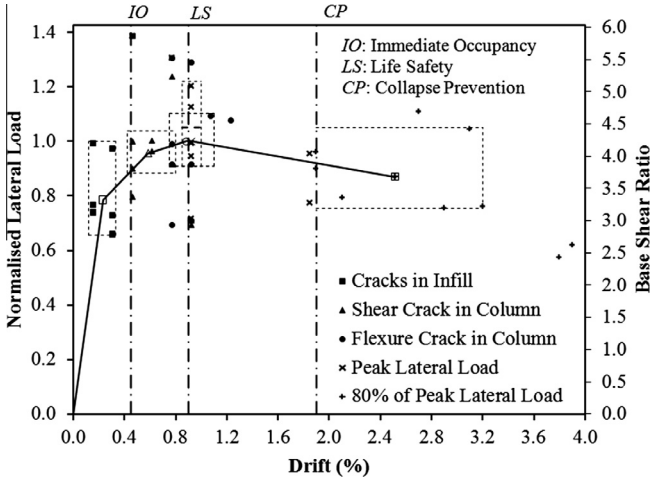

Fig. 11. Idealized load–displacement relationship for masonry infilled RC frames.

of 1.9–3.8%, with an average value of 2.6% [*COV* 0.24]; this can be regarded as ultimate limit state. The design drift level (0.4%) of the frame based on IS 1893 [27] was reached before the initiation of any major cracks in the frame elements at about 80% of the lateral strength of the infilled frame. Lateral drift values reported by Mehrabi et al. [6] for RC frames infilled with weak masonry were 0.17–0.36% for serviceability limit state, 1.02–1.88% for ultimate limit state, and 1.7–2.6% considering ultimate deformation. The lateral drift observed in the current study was significantly higher when compared to previous studies, due to the strong frame-weak infill configuration.

Based on these observations, three performance levels – *IO* (Immediate Occupancy), *LS* (Life Safety), and *CP* (Collapse Prevention) are suggested for the tested infilled RC frames. The performance level *IO* may be defined at a drift level of 0.45% before the onset of any major cracks (shear or flexure) in RC columns (infills may crack). According to ASCE 41, *IO* refers to minor cracking of both masonry infills and RC members followed by minor spalling of concrete cover. *LS* performance level may be defined at a drift level of 0.9% where significant shear cracks developed in columns and flexural cracks were initiated; at this level the lateral strength of the system was attained. ASCE 41 recommends *LS* level corresponding to extensive cracking and damage in infills and beams, and shear cracking in ductile columns. In the current study, *LS* is limited to cracking in infills and shear cracking in columns as no significant damage was observed in beams due to T-beam action. Since the lateral load behavior of infilled frames is quite brittle, *CP* performance level may be fixed at a drift level of 1.9% corresponding to initiation of significant drop in capacity (80% of lateral strength). According to ASCE 41, *CP* refers to extensive cracking and hinge formation in RC members. The idealized load–displacement curve proposed in the study is developed based on the limited study involving many uncertainties and the results need to be employed cautiously.

10. Summary and conclusions

Seismic design codes of many countries neglect the contribution of masonry infills in lateral load resistance and design RC frames as bare frames. On the other hand, a few national codes (IS 13920, Eurocode 8, and ASCE 41) have specific provisions for design and detailing of columns in such buildings. Effectiveness of such provisions in improving the lateral load behavior of infilled frames was assessed by carrying out an experimental study in two stages. In first stage, eight ductile and non-ductile frames, infilled with full-scale and half-scale bricks, were tested under slow cyclic lateral loads. And, three ductile frames designed and detailed for improved performance as per provisions of current seismic codes were tested in the second stage.

Results obtained in the first stage showed that infilled frames (using both full-scale and half-scale bricks) were significantly stiffer (7–10 times) and stronger (1.6–2.5 times), and dissipated more energy (1–2.3 times) than the corresponding bare frames. Though mortar to brick thickness was quite high in case of half-scale brick specimens, their lateral load behavior was quite similar to that of the specimens with full-scale bricks. The beneficial effect of ductile detailing in RC members was observed in the post peak regime of load–displacement curves in the form of gradual drop-down in capacity. At several instances (e.g., just after an earthquake) quick retrofitting of buildings is required to be carried out without detailed health assessment. In such cases, simple retrofitting strategy (replacing the damaged concrete, reinforcement, and infill) for infilled frames was found to be a viable option in restoring the original capacity.

It was further observed that though strong frame-weak infill configuration was used, columns of infilled frame failed in shear mode unlike past studies. Such brittle behavior is primarily attributed to weakening of interface connection between column and infill with increasing load that result in decreasing the effective length of column in contact with infill. This further increases the chord rotation demand leading to smaller shear span ratio and excessive shear demand on columns for which they were not designed. No significant damage was observed in beams of all specimens due to stiffening (T-beam) action provided by the RC slab.

In order to prevent/delay shear failure of RC columns, shear capacity of columns was enhanced in the second stage of the study following the recommendations of IS 13920, Eurocode 8 and ASCE 41. From the results, it was ascertained that using special confining reinforcement is beneficial in enhancing the lateral load behavior of infilled frames, especially in improving post-peak load behavior, energy dissipation, and ultimate deformation capacity. Though it was observed that initiation of shear cracks was delayed and the amount of shear cracks was lesser in the upgraded specimens, shear failure of columns could not be prevented. The provisions in current codes of practice do not seem to prevent the shear failure in RC columns of infilled frames, even when strong frame-weak infill configuration was used. An improved design method is required to be developed for RC columns of such frames.

An idealized load–displacement relationship was proposed based on the major damage events (performance levels) observed during the experimental study. This may serve as a guideline in the design of similar infilled frames for required performance levels. It is important to note that due care has to be taken while designing RC frames infilled with weak masonry, as they may also alter the failure mechanism of RC frame system.

Acknowledgements

Authors acknowledge the financial assistance provided by the Ministry of Human Resource Development (MHRD), and research grant (No. SR/FTP/ETA-22/08) provided by Department of Science and Technology, Government of India, under Fast Track Young Scientist Scheme. Specimens (1–4) were tested by Sagar Manchanda during his Master's program at IIT Guwahati.

References

[1] Moghaddam HA, Dowling PJ. The state art of the art in infilled frames. ESEE research report no 87-2. Civil Engineering Department, Imperial College of Science and Technology, London; 1987.
[2] Comite Euro-International Du Beton (CEB). RC frames under earthquake loading: state of the art report. Thomas Telford, London; 1996.
[3] Kaushik HB, Rai DC, Jain SK. Code approaches to seismic design of masonry infilled reinforced concrete frames: a state-of-the-art-review. Earthquake Spectra 2006;22(4):961–83.
[4] Asteris PG, Cotsovos DM. Numerical investigation of the effect of infill walls on the structural response of RC frames. Open Construct Build Technol J 2012;6:164–81. Bentham Science Publishers.
[5] Asteris PG, Cotsovos DM, Chrysostomou CZ, Mohebkhah A, Al-Chaar GK. Mathematical micromodeling of infilled frames: state of the art. Eng Struct 2013;56:1905–21. Elsevier.
[6] Mehrabi AB, Shing PB, Schuller MP, Noland JL. Experimental evaluation of masonry-infilled RC frames. J Struct Eng ASCE 1996;122(3):228–37.
[7] Al-Chaar G, Issa M, Sweeney S. Behavior of masonry–infilled nonductile reinforced concrete frames. J Struct Eng ASCE 2002;128(8):1055–63.
[8] Blackard B, William K, Mettupalayam S. Experimental observations of masonry infilled reinforced concrete frames with openings, vol. SP-265-9. ACI Special Publication; 2009. p. 199–222.
[9] Fardis MN. In: Seismic design, assessment and retrofitting of concrete buildings, based on EN-Eurocode 8. Series: geotechnical, geological and earthquake engineering, vol. 8. New York: Springer; 2009.
[10] Asteris PG, Antoniou ST, Sophianopoulos DS, Chrysostomou CZ. Mathematical macromodeling of infilled frames: state of the art. J Struct Eng ASCE 2011;137(12):1508–17.
[11] Markulak D, Radić I, Sigmund V. Cyclic testing of single bay steel frames with various types of masonry infill. Eng Struct 2013;51:267–77. Elsevier.
[12] Uva G, Porco F, Fiore A. Appraisal of masonry infill walls effect in the seismic response of RC framed buildings: a case study. Eng Struct 2012;34:514–26. Elsevier.

[13] Anil Ö, Altin S. An experimental study on reinforced concrete partially infilled frames. Eng Struct 2007;29(3):449–60. Elsevier.
[14] Ghosh AK, Amde AM. Finite element analysis of infilled frames. J Struct Eng ASCE 2002;128(7):881–9.
[15] El-Dakhakhni WW, Elgaaly M, Hamid AA. Three-strut model for concrete masonry-infilled frames. J Struct Eng ASCE 2003;129(2):177–85.
[16] European Committee of Standardization (CEN). Design of structures for earthquake resistance – Part 1: General rules, seismic actions and rules for buildings. EN 1998-1, Eurocode 8. Brussels; 2004.
[17] ASCE. Seismic evaluation and retrofit of existing buildings, ASCE/SEI 41–13. Reston, Virginia, USA; 2013.
[18] Masonry Standards Joint Committee (MSJC). Building code requirements and specifications for masonry structures. Farmington Hills, MI; 2013.
[19] Moretti ML, Papatheocharis T, Perdikaris PC. Design of reinforced concrete infilled frames. J Struct Eng ASCE 2014;140(9). 04014062(10).
[20] Celarec D, Dolšek M. Practice-oriented probabilistic seismic performance assessment of infilled frames with consideration of shear failure of columns. Earthquake Eng Struct Dyn 2013;42(9):1339–60.
[21] D'Ayala D, Worth J, Riddle O. Realistic shear capacity assessment of infill frames: comparison of two numerical procedures. Eng Struct 2009;31 (8):1745–61. Elsevier.
[22] Basha SH, Kaushik HB. Suitability of fly ash brick masonry as infill in reinforced concrete frames. Mater Struct 2015. http://dx.doi.org/10.1617/s11527-015-0757-. Springer in association with RILEM Publications.
[23] Tasnimi AA, Mohebkhah A. Investigation on the behavior of brick-infilled steel frames with openings, experimental and analytical approaches. Eng Struct 2011;33:968–80. Elsevier.
[24] Kakaletsis DJ, Karayannis CG. Influence of masonry strength and openings on infilled R/C frames under cycling loading. J Earthquake Eng 2008;12 (2):197–221.
[25] Zovkic J, Sigmund V, Guljas I. Cyclic testing of a single bay reinforced concrete frames with various types of masonry infill. Earthquake Eng Struct Dyn 2013;42(8):1131–49.
[26] Bureau of Indian Standards (BIS). Indian standard plain and reinforced concrete–code of practice, IS 456, 4th revision. New Delhi, India; 2000.
[27] Bureau of Indian Standards (BIS). Indian standard criteria for earthquake resistant design of structures. Part 1: General provisions and buildings, IS 1893. New Delhi, India; 2002.
[28] Bureau of Indian Standards (BIS). Indian standard ductile detailing of reinforced concrete structures subjected to seismic forces–code of practice, IS 13920. New Delhi, India; 1993.
[29] American Concrete Institute (ACI). Building code requirements for structural concrete. ACI 318; 2007.
[30] Basha SH, Kaushik HB. Evaluation of non-linear material properties of fly ash brick masonry under compression and shear. J Mater Civil Eng ASCE 2015;27 (8). http://dx.doi.org/10.1061/(ASCE)MT.1943-5533.000118. 04014227(1-11).
[31] Kaushik HB, Rai DC, Jain SK. Stress-strain characteristics of clay brick masonry under uniaxial compression. J Mater Civil Eng ASCE 2007;19(9):728–39.
[32] Asteris PG, Kakaletsis DJ, Chrysostomou CZ, Smyrou EE. Failure modes of in-filled frames. Electron J Struct Eng 2011;11:11–20.
[33] Mansouri A, Marefat MS, Khanmohammadi M. Experimental evaluation of seismic performance of low-shear strength masonry infills with openings in reinforced concrete frames with deficient seismic details. Struct Des Tall Spec Build 2014;23(15):1190–210.
[34] Chiou TC, Hwang SJ. Tests on cyclic behavior of reinforced concrete frames with brick infill. Earthquake Eng Struct Dyn 2015;44(12):1939–58.
[35] Stylianidis KC. Experimental investigation of masonry infilled R/C frames. Open Construct Build Technol J 2012;6(Suppl 1–M13):194–212.
[36] Kakaletsis DJ, Karayannis CG, Panagopoulos GK. Effectiveness of rectangular spiral shear reinforcement on infilled R/C frames under cyclic loading. J Earthquake Eng 2011;15(8):1178–93.
[37] Dizhur D, Ingham JM. Diagonal tension strength of vintage unreinforced clay brick masonry wall panels. Construct Build Mater 2013;43:418–27.
[38] Mainstone RJ. On the stiffnesses and strengths of infilled frames. Proc Inst Civil Eng 1971:57–90.